PHYSICAL REVIEW B **105**, 195148 (2022)

Relationship between electronic inhomogeneity and bandwidth in the organic conductor κ-(BEDT-TTF)$_2$Cu[N(CN)$_2$]I studied by ^{13}C NMR spectroscopy

T. Kobayashi,[1,*] A. Suzuta,[2] and A. Kawamoto[3]
[1]Graduate School of Science and Engineering, Saitama University, Saitama 338-8570, Japan
[2]Department of Physics, School of Science, Hokkaido University, Sapporo 060-0810, Japan
[3]Department of Condensed Matter Physics, Graduate School of Science, Hokkaido University, Sapporo 060-0810, Japan

(Received 2 October 2021; revised 19 April 2022; accepted 16 May 2022; published 31 May 2022)

In κ-(BEDT-TTF)$_2$Cu[N(CN)$_2$]X (X = Cl, Br) salts, where BEDT-TTF denotes bis(ethylenedithio)tetrathiafulvalene, the electronic properties can be characterized using a universal pressure-temperature phase diagram. Previous research [T. Kobayashi *et al.*, Phys. Rev. B **100**, 195115 (2019)] revealed a low-temperature insulating phase without antiferromagnetic ordering in the isostructural X = I (hereafter, κ-I) salt, which cannot be understood using the universal phase diagram. In addition, the κ-I salt naturally contains electronic inhomogeneity because of the development of a superlattice structure and/or disorder of the ethylene end groups. This could lead to physical properties that are different from those described by the universal phase diagram of κ-type salts. To investigate the relationship between the electronic inhomogeneity and universal phase diagram, ^{13}C NMR measurements were performed under pressure on this material. With increasing pressure, an increase in the bandwidth was revealed from a decrease in the Knight shift. The accompanying suppression of the inhomogeneity at low temperatures was evident from the linewidth. Once the inhomogeneity was suppressed, superconductivity was observed. The temperature dependence of the Knight shift and spin-lattice relaxation rate in the superconducting state is similar to that previously observed for κ-type salts, indicating that the symmetry of the superconducting gap is a d wave. When pressure was applied and the electronic inhomogeneity was suppressed, the physical properties of the κ-I salt were found to be qualitatively identical to those of the high-pressure side on the universal phase diagram. These results indicate that the ratio of electronic inhomogeneity to bandwidth is an essential parameter for this system.

DOI: 10.1103/PhysRevB.105.195148

I. INTRODUCTION

Superconductivity near the antiferromagnetic (AF) phase has been observed in many materials. This phenomenon is a central issue in strongly correlated electron systems [1]. Among them, the quasi-two-dimensional organic conductor κ-(BEDT-TTF)$_2$Cu[N(CN)$_2$]X (X = Cl, Br, I) has garnered significant attention because it exhibits unconventional superconductivity near the AF phase, and its electronic phase can be finely tuned by physical and chemical pressures, where BEDT-TTF is bis(ethylenedithio)tetrathiafulvalene. The X = Cl (hereafter κ-Cl) salt shows a transition from an AF insulator to a superconductor at approximately 30 MPa, so that the pressure-temperature (P-T) phase diagram has been determined precisely [2–4]. In the X = Br (κ-Br) salt, superconductivity emerges at ambient pressure [5] as the replacement of the halogen atom chlorine with bromine causes a chemical pressure effect. This enables us to study superconducting (SC) properties in detail [6]. These pressure effects can be understood by the change in U/W, where U is the on-site Coulomb interaction and W is the bandwidth [7]. Although these compounds have been studied intensively, only a few studies have focused on the X = I (κ-I) salt.

Because the crystal structure of the κ-I salt is identical to those of the κ-Cl and κ-Br salts [8], the properties of the κ-I salt should be characterized by the universal phase diagram. From the P-T phase diagram study of the κ-I salt [9], it exhibits an insulating behavior at ambient pressure and superconductivity below approximately 8 K under pressure. Because the SC critical pressure of the κ-I salt, ~0.1 GPa, is higher than that of the κ-Cl salt [2–4], the κ-I salt is expected to be located on the lower-pressure side of the universal phase diagram. However, the AF transition has not been observed in the κ-I salt [10,11]. These results suggest that a universal phase diagram cannot be used to characterize the physical properties of the κ-I salt.

In our previous ^{13}C-NMR study of the κ-I salt at ambient pressure [12], we found that the development of electronic inhomogeneity at low temperatures, which could be derived from the superlattice formation and/or the disorder of the ethylene end groups, suppresses the electronic coherency and keeps the system as an Anderson-type insulator without the AF ordering. Electron spin resonance and polarized femtosecond spectroscopy have also revealed that disorder has a significant effect on the electron system in the κ-I salt [13,14]. These results indicate that the effect of inhomogeneity on the κ-I salt conceals the inherent electronic properties of the κ-type salts, as expected from the universal phase diagram. Recently, it has been reported that the κ-Br and κ-Cl salts

---

[*] tkobayashi@phy.saitama-u.ac.jp

underwent drastic changes in the physical properties due to x-ray irradiation. The superconductivity of the κ-Br salt is entirely suppressed by x-ray irradiation, and insulating behavior is induced at low temperatures [15]. In the κ-Cl salt, x-ray irradiation for 500 h causes depression of the AF state, and the enhancement of the nuclear spin-lattice relaxation rate divided by the temperature $1/T_1T$ remains down to 0.4 K [16] as that observed in the κ-I salt [12]. Thus, the disorder effect could be an additional parameter controlling the physical properties of the κ-X (X = Cl, Br, I) salts. For a systematic understanding of the κ-X salts, the relationship between the disorder effect and the P-T phase diagram should be studied.

The study of the κ-I salt under pressure provides valuable insight into the effect of disorder on the universal phase diagram. This effect can be suppressed by applying pressure owing to the increase in W [17,18]. Because superconductivity emerges above 0.12 GPa in the κ-I salt [19], by applying pressure, the fluctuating AF phase with electronic inhomogeneity at ambient pressure is assumed to change into the inherent electronic phase described by the universal phase diagram. To determine whether the inherent electronic state of the κ-type salt is realized under pressure, we must also confirm the superconductivity characteristics of the κ-I salt.

NMR spectroscopy is a powerful probe for these purposes because it can measure the spin susceptibility from the Knight shift under pressure, which is directly correlated with W. The degree of spin inhomogeneity can be estimated from the linewidth of the NMR spectra. In other words, the pressure and disorder effects can be investigated simultaneously. In addition, the T_1 measurement allows us to measure magnetic fluctuations, which are essential for understanding the electronic states, and to discuss the symmetry of the SC gap. Therefore, we performed ^{13}C NMR measurements on the κ-I salt under pressure.

II. EXPERIMENTAL

Single crystals of κ-I salt were obtained using the electrochemical oxidation method [12]. For ^{13}C NMR measurements, we enriched a single side of the central C=C bond of the BEDT-TTF molecule with ^{13}C nuclei [20]. Hydrostatic pressure was applied using a NiCrAl-BeCu hybrid clamp cell with Daphne oil 7373 as the pressure medium. The pressure was applied at room temperature and calibrated at low temperatures. To confirm the superconductivity under pressure and verify its consistency with the previous results [9], SC transition temperatures T_c were determined from the change in the resonant frequency of the NMR tank circuit as a function of temperature at zero magnetic fields. As shown in Fig. 1(a), the measured T_c values are consistent with those determined by the end-junction point of resistivity [9]. Although some crystals of the κ-I salt exhibited filamentary superconductivity even at ambient pressure, the change in the resonant frequency indicates bulk superconductivity, which is consistent with the previous results [9,11]. The NMR measurements on a single crystal were performed at a magnetic field of 7 T parallel to the a axis, and shifts were measured relative to tetramethylsilane (TMS). The spectra were obtained by the fast Fourier transformation of the spin-echo signals following a $\pi/2$-π pulse sequence with a typical pulse length of 3 μs. The spin-lattice relaxation time, T_1, was measured using the conventional saturation recovery method. The spin-spin relaxation time T_2 was estimated using the exponential decay.

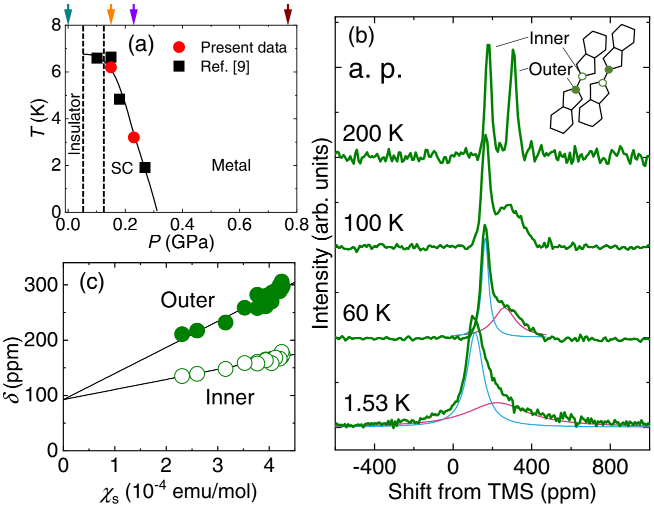

FIG. 1. (a) Pressure dependence of T_c compared with that reported in a previous study [9]. The region between the dashed lines represents the incomplete transition from insulator to superconductor. The arrows indicate the pressure at which the NMR experiments were performed. (b) Temperature evolution of the ^{13}C-NMR spectra at ambient pressure under a magnetic field of 7 T parallel to the a axis. Solid lines are fitted by two Lorentzians. Inset shows a dimer of BEDT-TTF molecules in the crystal of κ-I. Closed and open symbols represent ^{13}C enriched nuclei. There is an inversion center at the center of the dimer, and the sites near and far from it are assigned as inner and outer sites, respectively. (c) δ-χ_s plots of the outer and inner sites at ambient pressure. Solid lines are the results of the linear fitting.

III. RESULTS AND DISCUSSION

A. NMR shift

Figure 1(b) shows the temperature evolution of the NMR spectra of the κ-I salt at ambient pressure in the magnetic field parallel to the a axis. At 200 K, two NMR peaks were observed. In the κ-I salt, while the four dimers are magnetically inequivalent in the direction of an arbitrary magnetic field, they become magnetically equivalent in the direction of the a-axis magnetic field. As shown in the inset of Fig. 1(b), there are two sites per dimer, with the one closer to the center of the dimer assigned as the inner site and the one farther away as the outer site [12,21,22]. The observed peaks at 179 and 306 ppm correspond to the inner and outer sites, respectively. With decreasing temperature, the NMR shift decreases because of the decrease in the spin susceptibility, and the linewidth broadens. The low-temperature linewidth of the outer site becomes broader than that of the inner site, as reported previously [12].

The NMR shift, δ^i [i = inner (I), outer (O)], can be written as $\delta^i = A^i\chi_s + \sigma$, where A^i, χ_s, and σ are the hyperfine coupling constant, spin susceptibility, and chemical shift, respectively. To quantitatively discuss the temperature and pressure variations in χ_s, A^i and σ must be determined. Thus, δ^i at ambient pressure was plotted against χ_s (Ref. [12]),

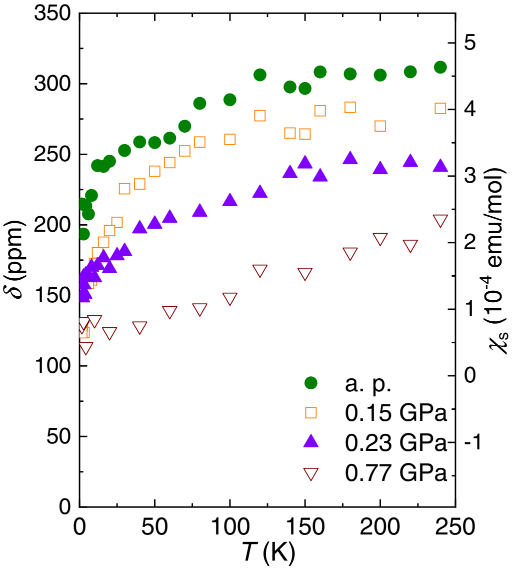

FIG. 2. Temperature dependence of NMR shift of outer site at various pressures. The local spin susceptibility χ_s is shown in the corresponding right scale.

as shown in Fig. 1(c). A^{I}, A^{O}, and σ were estimated to be (1.1 ± 0.1) kOe/μ_B, (2.6 ± 0.1) kOe/μ_B, and (93 ± 8) ppm, respectively. These results are consistent with those for isostructural κ-Br and κ-Cl salts [22,23].

Figure 2 shows the temperature dependence of δ^{O} at various pressures (left axis). χ_s, converted from $(\delta^{\mathrm{O}} - \sigma)/A^{\mathrm{O}}$, is also shown on the corresponding right axis. The temperature dependence of χ_s at ambient pressure in the a-axis magnetic field is consistent with those in the b and c axes, considering the sign of the hyperfine coupling constant [12]. χ_s at ambient pressure exhibits a weak temperature dependency at high temperatures and decreases considerably below ~15 K; this behavior can be interpreted as the development of AF fluctuations [12,24,25].

With increasing pressure, the absolute values of χ_s decrease, suggesting that applying pressure enhances W because $\chi_s \propto N(E_F)$ [$N(E_F)$: density of states at the Fermi energy] and $W \propto 1/N(E_F)$, that is, $\chi_s \propto 1/W$. These behaviors are similar to those of the κ-(BEDT-TTF)$_2$Cu(NCS)$_2$ (κ-NCS) salt. As pressure is applied to the κ-NCS salt [26], the absolute value of χ_s decreases. In addition, the temperature at which χ_s decreases shifts to a higher temperature. This corresponds to the temperature of the inflection point and its pressure change observed in electrical conductivity [27,28]. In the κ-I salt, the temperature at which χ_s decreases rapidly shifts to higher temperatures with increasing pressure. Eventually, at 0.77 GPa, χ_s decreases monotonically from 250 K to the lowest temperature by approximately 80 ppm, and a considerable decrease in χ_s was not observed. As in the case of the κ-NCS salt, the κ-I salt becomes metallic over the entire temperature range owing to pressurization [9], and the rapid decrease in χ_s is also suppressed.

As shown in the phase diagram in Fig. 1(a), the electrical conductivity is semiconducting at ambient pressure and metallic under pressure, which might suggest that the origin of χ_s is different at ambient and under pressure. However, even in the itinerant electronic states, semiconducting behavior can be realized, as in the bad metal state with short mean free paths. In this case, a continuous change of χ_s would be understood in the same itinerant electronic state, where the decreasing temperature of χ_s increases to a higher temperature continuously due to the pressure application, and the decreasing behavior also becomes less distinct.

B. Linewidth

The effect of the increase in W on the electronic inhomogeneity can be assessed from the linewidth. Figure 3(a) shows the NMR spectra at 4.2 K under pressures up to 0.77 GPa. Although the two peaks merge into a single line at all pressures, the linewidth of the outer site narrows with increasing pressure. To precisely examine the effect of pressure on the linewidth in frequency units ΔF, the temperature dependence of $\Delta F - \Delta F_{(T=240\ \mathrm{K})}$ for the outer site at various pressures is shown in Fig. 3(b). In addition to the ΔF derived from the electronic system, the inhomogeneity of the pressure distribution and magnetic field applied to the sample may also be the origin of ΔF. These are independent of the temperature, but the inhomogeneity of the pressure distribution depends on the pressure. Assuming that the ΔF derived from the electronic system is the same at high temperatures, where ΔF does not broaden, $\Delta F_{(T=240\ \mathrm{K})} = 2.1$ kHz (ambient pressure), 4.5 kHz (0.15 GPa), 4.0 kHz (0.23 GPa), and 5.6 kHz (0.77 GPa) were subtracted from the pressure dependence of the respective ΔF.

At ambient pressure, ΔF increases with decreasing temperature to 150 K, with a peak behavior of $1/T_2$ [Fig. 3(c)]. ΔF can be expressed as $\Delta F = (\gamma/2\pi)\Delta H + 1/T_2$, where γ and ΔH are the nuclear gyromagnetic ratio and static inhomogeneity of the local magnetic field at the nuclei, respectively. The second term can be used to detect slow fluctuations, and the observed $1/T_2$ peak at 150 K can be attributed to the dynamics of the ethylene end groups, as discussed previously [21,23,29]. Below 150 K, ΔF continues to increase, even though $1/T_2$ decreases, as observed for the κ-Br salt [21,30], suggesting that the line broadening below 150 K is due to static inhomogeneities. As discussed in our previous paper [12], the line broadening at approximately 70–150 K is not proportional to the hyperfine coupling constant in either the κ-Br or κ-I salts, indicating that line broadening is caused by mechanisms other than electronic inhomogeneity. The reason for the line broadening is attributed to the formation of the $c^*/2$ structure in the anion layer, which is commonly observed in κ-Br and κ-I salts [31,32]. As no anomalies were observed at approximately 150 K in χ_s and electrical conductivity [12], modulation of the anion layer, which does not affect the electronic system, can reasonably explain the line broadening.

We discuss the pressure effect on the line broadening down to ~100 K. The line broadening with the peak in $1/T_2$ does not change when the pressure is increased to 0.23 GPa. In the κ-Br salt, line broadening was observed to be independent of the pressure for up to 1 GPa [33]. The line broadening of the κ-I salt is qualitatively similar to that of the κ-Br salt, including the line broadening that is not correlated with the hyperfine coupling constant [12]. In addition, Shubnikov–de Haas oscillations and the Hall coefficients of the κ-Br salt

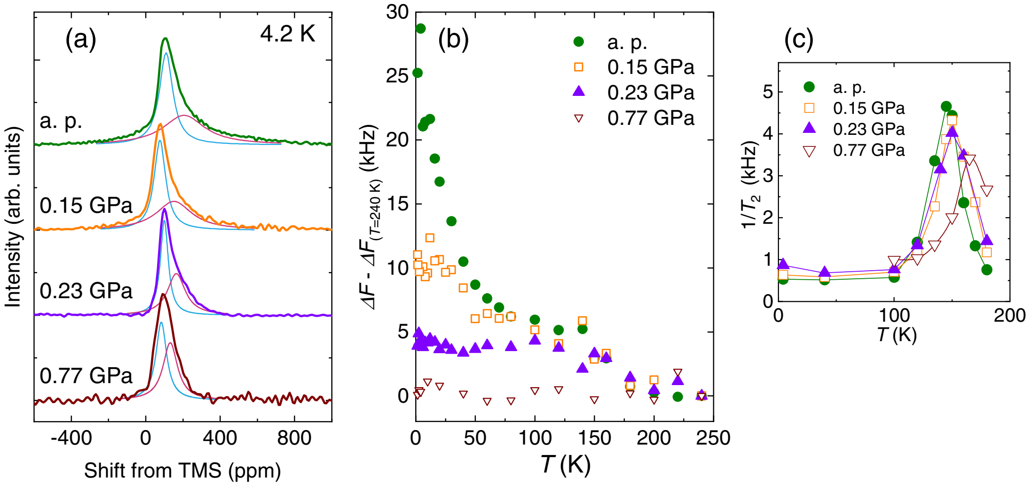

FIG. 3. (a) Pressure dependence of NMR shift at 4.2 K. The solid lines represent the fittings of the two Lorentzians. (b) Temperature dependence of $\Delta F - \Delta F_{(T=240\ \mathrm{K})}$ for the outer site under pressure. (c) Temperature dependence of $1/T_2$ on the outer site under pressure.

suggested doubling of the Fermi surface related to the $c^*/2$ structure, which does not change significantly with the application of pressure [34,35]. Therefore, the line broadening of the κ-I salt below 0.23 GPa in the high-temperature region can be attributed to the formation of the superlattice structure observed in the κ-Br salt.

At ambient pressure below 50 K, ΔF steeply increases, and the increase in ΔF is proportional to the hyperfine coupling constant [12]. This result indicates that the line broadening is due to the electronic inhomogeneity. While line broadening above 50 K is insensitive to pressure, the line broadening below 50 K is significantly suppressed owing to the applied pressure. Although line broadening was still observed at 0.15 GPa below 50 K, the degree of broadening is suppressed compared with that at ambient pressure. At 0.23 GPa, additional line broadening was not observed below 100 K, and its temperature dependence is similar to that of the κ-Br salt [30].

At 0.15 and 0.23 GPa, the line broadening below 50 K was suppressed by applying pressure, and superconductivity was realized [Fig. 1(b)]. These results suggest that the suppression of electronic inhomogeneity is essential for inducing superconductivity. We believe that the application of pressure increases W and enhances the coherency of electrons, relatively suppressing electron inhomogeneity in the κ-I salt. As a result, the P-T phase diagram as in the κ-Br salt is realized.

C. Spin-lattice relaxation rate

1. Paramagnetic state

Based on the results of the NMR shift and linewidth, the electronic inhomogeneity below 50 K was suppressed by an increase in W with the application of pressure. When such a change in the electronic state occurs, the magnetic fluctuations that characterize the dynamic magnetic properties of the κ-type salt are of interest and can be investigated by T_1 measurements. Because there are two independent ^{13}C sites under the a-axis magnetic field, T_1 at all temperatures was obtained by integrating the NMR intensities of both the inner and outer sites and by fitting the relaxation curve with two stretched exponential functions [36,37], $1 - M(t)/M(\infty) = \frac{1}{2}\exp[-(t/T_1^{\mathrm{O}})^{\beta}] + \frac{1}{2}\exp[-(t/T_1^{\mathrm{I}})^{\beta}]$, where $T_1^{\mathrm{I}}/T_1^{\mathrm{O}} = 3$. Here, $M(t)$ and $M(\infty)$ are the nuclear magnetization at time t after saturation and the equilibrium nuclear magnetization at $t \to \infty$, respectively. β is a stretching exponent that characterizes the distribution of relaxation. T_1^{I} and T_1^{O} are the T_1 of the inner and outer sites, respectively, and their ratios were determined from the average of the measurements at high temperatures where the peaks clearly split. In the following, we evaluate T_1 as T_1^{I}.

The relaxation profiles in the inhomogeneous electronic state can be described by the stretched exponential function. To cross-check the suppression of inhomogeneity, the temperature dependence of β at various pressures is plotted in Fig. 4(a). Above approximately 50 K, although the data points are scattered, β is close to unity at all pressures, indicating that the electronic system is homogeneous. Below 50 K, β decreases monotonically with decreasing temperature at ambient pressure and 0.15 GPa, while β is almost unity at 0.23 and 0.77 GPa. These results are consistent with the fact that the low-temperature line broadening remains below 0.15 GPa and is suppressed above 0.23 GPa.

Figure 4(b) shows the temperature dependence of $1/T_1T$ at several pressures. At ambient pressure, $1/T_1T$ increases with decreasing temperature, and the increase in $1/T_1T$ becomes less pronounced at 30 K. Below 15 K, $1/T_1T$ increases steeply again, with an increase of an order of magnitude when the temperature decreases to 1.5 K, as shown in the inset of Fig. 4(b). We suggested that the increase in $1/T_1T$ at low temperatures is due to the development of AF fluctuation, in which the electronic inhomogeneity suppresses the development of coherency and the Anderson-type insulating behavior persists down to the lowest temperature [12], as observed in the x-ray irradiated κ-Cl salt [16].

At 0.15 GPa, $1/T_1T$ exhibits a hump structure at approximately 40 K and increases again below 15 K. This temperature seems to correspond to the temperature at which $1/T_1T$ begins

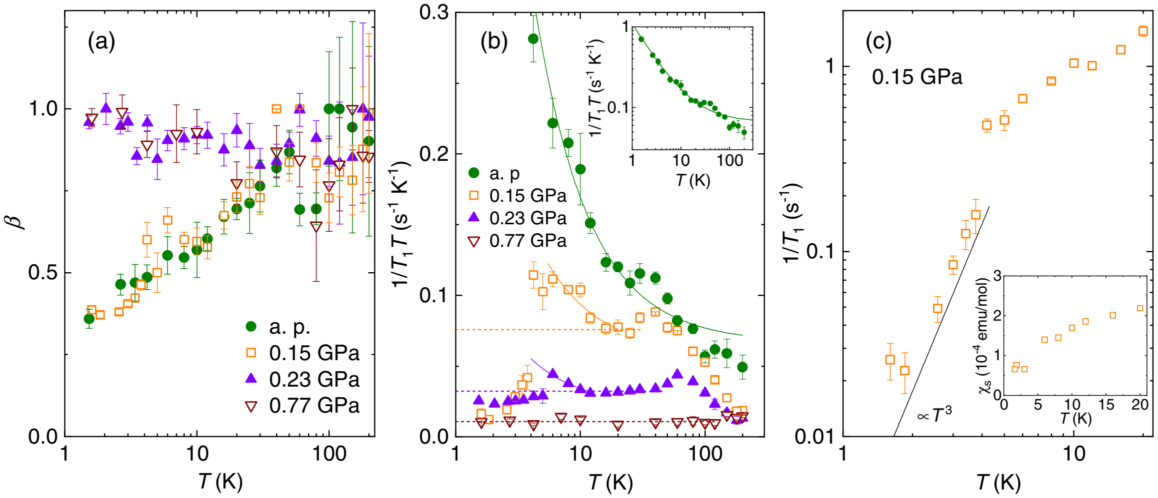

FIG. 4. (a) Temperature dependence of stretched exponent β at various pressures. (b) Temperature dependence of $1/T_1T$ at various pressures. Because $1/T_1T$ at ambient pressure drastically increases at low temperatures, the entire behavior is shown in the inset. Solid lines are fitting by $C/T + k$. The dashed lines are the average values in the region where $1/T_1T$ is constant. (c) Temperature dependence of $1/T_1$ at 0.15 GPa in the SC state. The solid line denotes the T^3 dependence. Inset shows the temperature dependence of χ_s estimated from the NMR shift.

to increase steeply at ambient pressure. Below 7 K, $1/T_1T$ drastically decreases because of the SC transition discussed in Sec. III C 2.

At 0.23 GPa, the linewidth is similar to that of the κ-Br salt, where the electronic inhomogeneity below 50 K is suppressed. β does not change significantly at low temperatures, demonstrating a homogeneous electronic distribution. $1/T_1T$ at 0.23 GPa increases with decreasing temperature from 200 K, as does that at 0.15 GPa, but begins to decrease below 60 K and becomes constant in the range of approximately 10–40 K. Although $1/T_1T$ at ambient pressure continues to increase below 200 K, at 0.15 and 0.23 GPa, this increase is suppressed. This differs from the behavior of $1/T_1T$ in $(\mathrm{TMTSF})_2\mathrm{PF}_6$, for which the non-Fermi-liquid state and the possibility of superconductivity near the quantum critical point have been discussed [38,39]. On the other hand, a similar behavior has been observed in the κ-Br salt, where the peaks of $1/T_1T$ at $T^* = 50$ K and $1/T_1T =$ constant below T^* have been observed, indicating that the Fermi liquid state was realized below T^* [40]. T^* corresponds to the temperature at which the electrical resistance exhibits an inflection point, suggesting a crossover from the bad metal to the Fermi liquid state [41]. The peak of $1/T_1T$ is considered to arise from the suppression of spin fluctuations, which originate from the AF ordering in the κ-Cl salt, owing to the development of itinerancy. In the κ-I salt, a slope change in the electrical resistance under pressure was observed at the corresponding temperature [9]. Therefore, the peak of $1/T_1T$ at 0.23 GPa is interpreted to be due to the same T^* anomaly as in the κ-Br salt, which is characteristic of κ-type superconductors in the vicinity of the AF phase.

Because $T^* = 60$ K of the κ-I salt at 0.23 GPa is higher than that of the κ-Br and κ-NCS salts [40], the κ-I salt at 0.23 GPa is considered to be located on the high-pressure side compared with the κ-Br and κ-NCS salts in the universal phase diagram. The results of the NMR shifts provide consistent conclusions. At ambient pressure, χ_s is almost the same for the κ-Br and κ-I salts above 50 K [12], indicating nearly the same W for the κ-Br and κ-I salts. From the NMR shifts under pressure, χ_s decreases with increasing pressure; therefore, the κ-I salt at 0.23 GPa has a larger W than that at ambient pressure and corresponds to the pressurized κ-Br and κ-NCS salts. In fact, the application of pressure shifts the temperature of T^* in the κ-NCS salt to a higher temperature and decreases χ_s [26]. Considering the pressure variation in T^*, the peak at 40 K observed at 0.15 GPa can also be interpreted as the T^* anomaly.

As discussed above, the $1/T_1T$ of 0.23 GPa is similar to that of the κ-Br salt. However, an additional increase in $1/T_1T$ below 10 K was not observed for the other κ-type salts. This could be related to the steeper increase in $1/T_1T$ at 0.15 GPa observed below 15 K. At 0.15 GPa, $1/T_1T$ and the Knight shift decrease with the SC transition; however, at 0.23 GPa, there is no significant change in the Knight shift, suggesting that the origin of the decrease in $1/T_1T$ is different for both pressures. Details will be discussed in Sec. III E.

From 0.15 GPa, where the $1/T_1T =$ constant behavior was observed, the temperature range of $1/T_1T =$ constant expands, and its value decreases as the pressure increases [dashed lines in Fig. 4(b)]. At 0.77 GPa, the significant temperature dependence of $1/T_1T$ is eventually suppressed over the entire temperature range, suggesting that the system is far from the AF phase. The constant values of $1/T_1T$, $(1/T_1T)_{\mathrm{FL}}$, at each pressure are listed in Table I along with T_c. When T_c is decreased by approximately half from 0.15 GPa to 0.23 GPa, the $(1/T_1T)_{\mathrm{FL}}$ values also decreased to a similar extent, suggesting a correlation between them. A similar decrease in $(1/T_1T)_{\mathrm{FL}}$ was also observed for the κ-Br and κ-NCS salts [26,42]. In particular, in the κ-NCS salt, the correlation between T_c and the Korringa factor has been reported [26]. These similar behaviors indicate that the κ-I salt, whose electronic inhomogeneity is suppressed by pressure, can be comprehended using the universal phase diagram.

TABLE I. SC transition temperature T_c, $1/T_1T$ = constant values below T^* [$(1/T_1T)_{\rm FL}$], and parameters obtained by fitting $1/T_1T$ at low temperatures with $C/T + k$ for each pressure.

P (GPa)	T_c (K)	$(T_1T)^{-1}_{\rm FL}$ ($\rm s^{-1}\ K^{-1}$)	C ($\rm s^{-1}$)	k
ambient pressure	n/a	n/a	1.02(6)	0.067(4)
0.15	6.2	0.075(2)	0.35(7)	0.059(7)
0.23	3.2	0.032(1)	0.14(2)	0.020(2)
0.77	n/a	0.011(2)	n/a	n/a

2. *Superconducting state*

We found that the inherent physical properties of κ-type salts expected from the universal phase diagram appear by applying pressure to increase W and suppress electronic inhomogeneity. In addition, superconductivity appears immediately once the inhomogeneity is suppressed. It is essential to investigate whether the properties of this superconductivity are the same as those of the other κ-type superconductors. As mentioned in Sec. II, T_c was confirmed at a zero magnetic field (Table I). In the T_1 measurements, superconductivity was not observed at 0.23 GPa, whereas a drastic decrease in $1/T_1T$ resulting from the SC ordering was observed at 0.15 GPa. This is because at 0.23 GPa, T_c is lower, and the applied magnetic field of 7 T exceeds the upper critical field H_{c2}, whereas at 0.15 GPa, T_c is higher, and H_{c2} is sufficiently higher than the applied field. In fact, H_{c2} parallel to the conduction plane at 0.12 GPa is approximately 15 T, as determined by electrical resistivity measurements [9]. Thus, we can discuss the results of NMR measurements in the SC state at 0.15 GPa semiquantitatively.

Figure 4(c) shows the temperature dependence of $1/T_1$ in the SC state. Immediately below 4 K, $1/T_1$ drastically decreases without indicating a coherence peak, while it decreases according to the T^3 dependence at low temperatures. Although a field of 7 T may suppress the coherence peak, the T^3 dependence is a characteristic behavior of superconductors with line nodes. The inset in Fig. 4(c) shows the temperature dependence of χ_s, estimated from the NMR shift. We also found that χ_s decreases below 5 K, indicating a spin-singlet state. The temperature at which $1/T_1$ and Knight shift decrease abruptly agrees with the reported T_c in the corresponding magnetic field at 0.12 GPa (T_c is nearly the same as that at 0.15 GPa) [9]. These features are identical to those of the κ-Br salt and can be understood by the spin-singlet d-wave SC gap symmetry [30,43,44]. Therefore, the SC property of the κ-I salt is the same as that of typical κ-type salts.

D. Effect of inhomogeneity in the *P-T* phase diagram

When pressure was applied, line broadening was immediately suppressed, leading to superconductivity. Hence, the suppression of electronic inhomogeneity is crucial for the realization of superconductivity. We discuss the relationship between the effects of electronic inhomogeneity and the P-T phase diagram. Experimentally, the W values of κ-X (X = Cl, Br, I) salts are comparable [12]. However, the interdimer transfer integrals of the κ-I salt, which are estimated from the crystal structure, are smaller than those of κ-Br and κ-Cl salts [45–47]. In the κ-I salt, an additional superstructure of $c^*/3$ below 100 K has been reported and suggested to be related to the emergence of superconductivity [9,32]. The superstructure leads to a disorder potential, D. Hence, the ratio of D/W in the κ-I salt is larger than that in κ-Br and κ-Cl salts, and a relatively large D/W induces electronic inhomogeneity. In the κ-I salt, the inherent physical properties of κ-type salts can be easily masked by electronic inhomogeneity. The increase in W with only a small application of pressure could overcome the electronic inhomogeneity. Therefore, the ratio of D/W should be an additional parameter, along with the pressure (U/W) and temperature, which can help understand the physical properties of κ-type salts.

The physical properties of the κ-I salt can be characterized by the P-T phase diagram of the inherent κ-type salt above the pressure at which inhomogeneity is suppressed. By applying a pressure of 0.23 GPa to the κ-I salt, the linewidth becomes comparable to that of the κ-Br salt, suggesting that the inhomogeneity is sufficiently suppressed. Consequently, the $1/T_1T$ behavior of the κ-I salt is the same as that of the κ-Br salt. When 0.77 GPa was applied, the AF fluctuations were suppressed, and the superconductivity disappeared.

E. Distinctive feature of κ-I salt

The results at 0.15 and 0.23 GPa indicate that the electronic inhomogeneity below 50 K is suppressed by the application of pressure, resulting in the existence of T^*, Fermi-liquid-like behavior below T^*, and the possibility of d-wave superconductivity, which is similar to the behavior of the κ-Br salt [40,43]. However, unlike the κ-Br salt, $1/T_1T$ increased slightly below 15 K (immediately above T_c) at 0.15 and 0.23 GPa. As shown in Fig. 4(a), homogeneous relaxation was observed at 0.23 GPa, indicating that the increase in $1/T_1T$ is intrinsic. To understand the increasing trend of $1/T_1T$, we fitted the temperature dependence of $1/T_1T$ with $C/T + k$ for pressures up to 0.23 GPa. Here, C is the Curie constant and k is a constant term. Note that we attempted to include the Weiss temperature in the analysis; however, because it had no reliable accuracy and was almost zero, it was neglected here. At ambient pressure, because there is no T^* anomaly and κ-I salt is semiconducting, we fitted $1/T_1T$ below 200 K. Under pressure, $1/T_1T$ was fitted below the temperature at which it deviated from the $(1/T_1T)_{\rm FL}$ values at low temperatures. The fitting parameters for each pressure are presented in Table I. In the SC state, there are only results for two pressure points, but C and T_c might be related.

While the above discussion suggests that the increase in $1/T_1T$ at low temperatures is related to the mechanism of superconductivity, there are two possible interpretations of the increase in $1/T_1T$: one is that the AF fluctuation observed at ambient pressure enhances again under pressure below 15 K, and the other is that the magnetic fluctuation from a different AF instability appears. Unlike neutron diffraction experiments, NMR detects the sum of magnetic fluctuations at all wave numbers as $1/T_1T$, and thus magnetic fluctuations at ambient pressure and those under pressure cannot be distinguished experimentally. Recently, in the λ-(BETS)$_2$GaCl$_4$ salt, the existence of T^*, Fermi-liquid-like behavior below T^*, and the possibility of d-wave superconductivity have been suggested [48,49]. In addition, an increase in $1/T_1T$ was observed just above the superconductivity [48], which can be explained by the spin-density-wave (SDW) fluctuation because the SDW state was found in the vicinity of the SC phase [50]. The possibility of spin-fluctuation-mediated superconductivity related to the Fermi surface nesting has been suggested in κ-type salts [51], and the correlation between the Korringa factor and T_c has been reported [26]. In the κ-I salt, the timescale of the SDW fluctuation could be in the NMR frequency range, which might cause an increase in $1/T_1T$ at low temperatures. Currently, this scenario is only speculative; however, we believe it is informative to search for the existence of a magnetically ordered state near the phase diagram of κ-I salt that is different from κ-Cl salt.

Finally, we consider the line broadening at approximately 100–200 K observed for both the κ-Br and κ-I salts. This anomaly was not observed in κ-Cl and κ-NCS salts [23,29], and has no significant effect on the electronic system, suggesting a superlattice structure in the anion layer [9]. It is noteworthy that in the κ-I salt at 0.77 GPa, the line broadening below 200 K appears to be suppressed. However, it has been pointed out that the superlattice structure of the κ-Br salt does not disappear even at 1 GPa [34,35]. To verify the connection between the superlattice structure and line broadening, determining whether the superlattice structure of the κ-I salt exists at a pressure of 0.77 GPa is necessary. If the superlattice structure of $c^*/2$ disappears at 0.77 GPa, we can conclude that the line broadening of the κ-Br and κ-I salts at 150 K is related to the $c^*/2$ structure.

IV. SUMMARY

In conclusion, we performed the ^{13}C NMR measurements on κ-I salt under various pressures to investigate the relationship between the disorder effect and the universal phase diagram established for the κ-Br, κ-Cl, and κ-NCS salts. The application of pressure decreases the spin susceptibility, which is proportional to the inverse of the bandwidth, and suppresses the line broadening at low temperatures because of the electronic inhomogeneity. The suppression of electronic inhomogeneity is crucial for the realization of superconductivity. In the T_1 measurement, immediately after the suppression of the electronic inhomogeneity, the physical properties described by the universal phase diagram, T^* anomaly, Fermi-liquid-like behavior, and d-wave superconductivity were observed. From these results, we propose that in addition to the parameters of U/W and temperature, the ratio of the disorder to bandwidth D/W is important for a deep understanding of the universal phase diagram. In addition, we observed an increase in $1/T_1T$ below 15 K just above T_c, which was not predicted from the previous universal phase diagram.

ACKNOWLEDGMENTS

We thank Y. Ihara (Hokkaido University) for his advice on setting up the pressure cell. This work was partially supported by the Japan Society for the Promotion of Science KAKENHI Grants No. 20K14401 and No. 19K03758.

[1] K. H. Bennemann and J. B. Ketterson, editors, *Superconductivity* (Springer, Berlin, 2008).

[2] S. Lefebvre, P. Wzietek, S. Brown, C. Bourbonnais, D. Jérome, C. Mézière, M. Fourmigué, and P. Batail, Mott Transition, Antiferromagnetism, and Unconventional Superconductivity in Layered Organic Superconductors, Phys. Rev. Lett. **85**, 5420 (2000).

[3] P. Limelette, P. Wzietek, S. Florens, A. Georges, T. A. Costi, C. Pasquier, D. Jérome, C. Mézière, and P. Batail, Mott Transition and Transport Crossovers in the Organic Compound κ-(BEDT-TTF)$_2$Cu[N(CN)$_2$]Cl, Phys. Rev. Lett. **91**, 016401 (2003).

[4] F. Kagawa, K. Miyagawa, and K. Kanoda, Unconventional critical behaviour in a quasi-two-dimensional organic conductor, Nature (London) **436**, 534 (2005).

[5] A. M. Kini, U. Geiser, H. H. Wang, K. D. Carlson, J. M. Williams, W. K. Kwok, K. G. Vandervoort, J. E. Thompson, D. L. Stupka, D. Jung, and M.-H. Whangbo, A new ambient-pressure organic superconductor, κ-(ET)$_2$Cu[N(CN)$_2$]Br, with the highest transition temperature yet observed (inductive onset $T_c = 11.6$ K, resistive onset = 12.5 K), Inorg. Chem. **29**, 2555 (1990).

[6] K. Miyagawa, K. Kanoda, and A. Kawamoto, NMR studies on two-dimensional molecular conductors and superconductors: Mott transition in κ-(BEDT-TTF)$_2X$, Chem. Rev. **104**, 5635 (2004).

[7] K. Kanoda, Recent progress in NMR studies on organic conductors, Hyperfine Interact. **104**, 235 (1997).

[8] U. Geiser, A. J. Schults, H. H. Wang, D. M. Watkins, D. L. Stupka, J. M. Williams, J. E. Schirber, D. L. Overmyer, D. Jung, J. J. Novoa, and M.-H. Whangbo, Strain index, lattice softness and superconductivity of organic donor-molecule salts, Physica C: Superconductivity **174**, 475 (1991).

[9] M. A. Tanatar, T. Ishiguro, S. Kagoshima, N. D. Kushch, and E. B. Yagubskii, Pressure-temperature phase diagram of the organic superconductor κ-(BEDT-TTF)$_2$Cu[N(CN)$_2$]I, Phys. Rev. B **65**, 064516 (2002).

[10] V. Kataev, G. Winkel, D. Khomskii, D. Wohlleben, W. Crump, K. Tebbe, and J. Hahn, ESR of single crystals of κ-(BEDT-TTF)$_2$Cu[N(CN)$_2$]X (X = Br and I), Solid State Commun. **83**, 435 (1992).

[11] V. Kataev, G. Winkel, N. Knauf, A. Gruetz, D. Khomskii, D. Wohlleben, W. Crump, J. Hahn, and K. Tebbe, ESR study of the electronic properties of the new organic conductors κ-(BEDT-TTF)$_2$Cu[N(CN)$_2$]X, X = Br; I, Phys. B: Condens. Matter **179**, 24 (1992).

[12] T. Kobayashi, A. Suzuta, K. Tsuji, Y. Ihara, and A. Kawamoto, Inhomogeneous electronic state of organic conductor κ-(BEDT-TTF)$_2$Cu[N(CN)$_2$]I studied by ^{13}C NMR spectroscopy, Phys. Rev. B **100**, 195115 (2019).

[13] L. N. Majer, B. Miksch, O. Iakutkina, T. Kobayashi, A. Kawamoto, and M. Dressel, Interacting electron spins in κ-(BEDT-TTF)$_2$Cu[N(CN)$_2$]I investigated by ESR spectroscopy, Phys. Rev. B **102**, 214430 (2020).

[14] S. Tsuchiya, R. Kuwae, T. Kodama, Y. Nakamura, M. Kurihara, T. Yamamoto, T. Naito, and Y. Toda, Electronic inhomogeneity

in organic charge transfer salt κ-(BEDT-TTF)$_2$Cu[N(CN)$_2$]I probed by polarized femtosecond spectroscopy, J. Phys. Soc. Jpn. **89**, 064712 (2020).

[15] K. Sano, T. Sasaki, N. Yoneyama, and N. Kobayashi, Electron Localization near the Mott Transition in the Organic Superconductor κ-(BEDT-TTF)$_2$Cu[N(CN)$_2$]Br, Phys. Rev. Lett. **104**, 217003 (2010).

[16] T. Furukawa, K. Miyagawa, T. Itou, M. Ito, H. Taniguchi, M. Saito, S. Iguchi, T. Sasaki, and K. Kanoda, Quantum Spin Liquid Emerging from Antiferromagnetic Order by Introducing Disorder, Phys. Rev. Lett. **115**, 077001 (2015).

[17] A. Kawamoto, Y. Honma, K.-i. Kumagai, N. Matsunaga, and K. Nomura, Suppression of inhomogeneous electron localization in κ-(BEDT-TTF)$_2$Cu$_2$(CN)$_3$ under pressure, Phys. Rev. B **74**, 212508 (2006).

[18] Y. Eto, M. Itaya, and A. Kawamoto, Non-Fermi-liquid behavior of the organic superconductor κ-(BEDT-TTF)$_4$Hg$_{2.89}$Br$_8$ probed by ^{13}C NMR, Phys. Rev. B **81**, 212503 (2010).

[19] N. D. Kushch, M. A. Tanatar, E. B. Yagubskii, and T. Ishiguro, Superconductivity of κ-(BEDT-TTF)$_2$Cu[N(CN)$_2$]I under pressure, JETP Lett. **73**, 429 (2001).

[20] S. Hirose, M. Misawa, and A. Kawamoto, Magnetic and electric properties of organic conductors probed by ^{13}C-NMR using selective-site substituted molecules, Crystals **2**, 1034 (2012).

[21] S. M. De Soto, C. P. Slichter, A. M. Kini, H. H. Wang, U. Geiser, and J. M. Williams, ^{13}C NMR line-shape studies of the organic superconductor κ-(ET)$_2$Cu[N(CN)$_2$]Br, Phys. Rev. B **54**, 16101 (1996).

[22] Y. Saito and A. Kawamoto, Determination of the hyperfine coupling tensor in organic conductors κ-(BEDT-TTF)$_2X$ (X = Cu[N(CN)$_2$]Br, Cu(NCS)$_2$) on central ^{13}C sites, Solid State Nucl. Magn. Reson. **73**, 22 (2016).

[23] M. Matsumoto, Y. Saito, and A. Kawamoto, Molecular motion and high-temperature paramagnetic phase in κ-(BEDT-TTF)$_2$Cu[N(CN)$_2$]Cl, Phys. Rev. B **90**, 115126 (2014).

[24] T. Sasaki, N. Yoneyama, A. Matsuyama, and N. Kobayashi, Magnetic and electronic phase diagram and superconductivity in the organic superconductors κ-(ET)$_2X$, Phys. Rev. B **65**, 060505(R) (2002).

[25] N. Yoneyama, T. Sasaki, and N. Kobayashi, Magnetic phase diagram and superconductivity in κ-type ET salts, Synth. Met. **137**, 1205 (2003).

[26] M. Itaya, Y. Eto, A. Kawamoto, and H. Taniguchi, Antiferromagnetic Fluctuations in the Organic Superconductor κ-(BEDT-TTF)$_2$Cu(NCS)$_2$ under Pressure, Phys. Rev. Lett. **102**, 227003 (2009).

[27] K. Murata, M. Tokumoto, H. Anzai, Y. Honda, N. Kinoshita, T. Ishiguro, N. Toyota, T. Sasaki, and Y. Muto, Superconductivity of BEDT-TTF salts: (I) Effect of pressure and alloying and (II) Shubnikov–de Haas effect, Synth. Met. **27**, A263 (1988).

[28] K. Murata, M. Ishibashi, Y. Honda, N. A. Fortune, M. Tokumoto, N. Kinoshita, and H. Anzai, Temperature dependence of Hall effect in κ-(BEDT-TTF)$_2$Cu(NCS)$_2$, Solid State Commun. **76**, 377 (1990).

[29] Y. Kuwata, M. Itaya, and A. Kawamoto, Low-frequency dynamics of κ-(BEDT-TTF)$_2$Cu(NCS)$_2$ observed by ^{13}C NMR, Phys. Rev. B **83**, 144505 (2011).

[30] S. M. De Soto, C. P. Slichter, A. M. Kini, H. H. Wang, U. Geiser, and J. M. Williams, ^{13}C NMR studies of the normal and superconducting states of the organic superconductor κ-(ET)$_2$Cu[N(CN)$_2$]Br, Phys. Rev. B **52**, 10364 (1995).

[31] Y. Nogami, J. P. Pouget, H. Ito, T. Ishiguro, and G. Saito, Superlattice structural transition in the organic superconductor κ-(BEDT-TTF)$_2$Cu[N(CN)$_2$]Br, Solid State Commun. **89**, 113 (1994).

[32] M. A. Tanatar, S. Kagoshima, T. Ishiguro, H. Ito, V. S. Yefanov, V. A. Bondarenko, N. D. Kushch, and E. B. Yagubskii, Electronic transport properties and structural transformations of κ-(BEDT-TTF)$_2$Cu[N(CN)$_2$]I, Phys. Rev. B **62**, 15561 (2000).

[33] Y. Kuwata, ^{13}C-NMR study on slow dynamics of ethylene groups in κ-(BEDT-TTF)$_2X$, Master's thesis, Hokkaido University, 2011.

[34] H. Weiss, M. V. Kartsovnik, W. Biberacher, E. Steep, E. Balthes, A. G. M. Jansen, K. Andres, and N. D. Kushch, Magnetotransport studies of the Fermi surface in the organic superconductor κ-(BEDT-TTF)$_2$Cu[N(CN)$_2$]Br, Phys. Rev. B **59**, 12370 (1999).

[35] K. Katayama, T. Nagai, H. Taniguchi, K. Satoh, N. Tajima, and R. Kato, High-pressure electronic state of κ-(BEDT-TTF)$_2$Cu[N(CN)$_2$]Br probed by Hall effect, J. Phys. Soc. Jpn. **76**, 194 (2007).

[36] T. Kobayashi, Y. Ihara, Y. Saito, and A. Kawamoto, Microscopic observation of superconducting fluctuations in κ-(BEDT-TTF)$_2$Cu[N(CN)$_2$]Br by ^{13}C NMR spectroscopy, Phys. Rev. B **89**, 165141 (2014).

[37] T. Kobayashi, Y. Ihara, and A. Kawamoto, Modification of local electronic state by BEDT-STF doping to κ-(BEDT-TTF)$_2$Cu[N(CN)$_2$]Br salt studied by ^{13}C NMR spectroscopy, Phys. Rev. B **93**, 094515 (2016).

[38] N. Doiron-Leyraud, P. Auban-Senzier, S. René de Cotret, C. Bourbonnais, D. Jérome, K. Bechgaard, and L. Taillefer, Correlation between linear resistivity and T_c in the Bechgaard salts and the pnictide superconductor Ba(Fe$_{1-x}$Co$_x$)$_2$As$_2$, Phys. Rev. B **80**, 214531 (2009).

[39] Y. Kimura, M. Misawa, and A. Kawamoto, Correlation between non-Fermi-liquid behavior and antiferromagnetic fluctuations in (TMTSF)$_2$PF$_6$ observed using ^{13}C-NMR spectroscopy, Phys. Rev. B **84**, 045123 (2011).

[40] A. Kawamoto, K. Miyagawa, Y. Nakazawa, and K. Kanoda, ^{13}C NMR Study of Layered Organic Superconductors Based on BEDT-TTF Molecules, Phys. Rev. Lett. **74**, 3455 (1995).

[41] C. Strack, C. Akinci, V. Paschenko, B. Wolf, E. Uhrig, W. Assmus, M. Lang, J. Schreuer, L. Wiehl, J. A. Schlueter, J. Wosnitza, D. Schweitzer, J. Müller, and J. Wykhoff, Resistivity studies under hydrostatic pressure on a low-resistance variant of the quasi-two-dimensional organic superconductor κ-(BEDT-TTF)$_2$Cu[N(CN)$_2$]Br: Search for intrinsic scattering contributions, Phys. Rev. B **72**, 054511 (2005).

[42] H. Mayaffre, P. Wzietek, C. Lenoir, D. Jérome, and P. Batail, ^{13}C NMR study of a quasi-two-dimensional organic superconductor κ-(ET)$_2$Cu[N(CN)$_2$]Br, Europhys. Lett. **28**, 205 (1994).

[43] H. Mayaffre, P. Wzietek, D. Jérome, C. Lenoir, and P. Batail, Superconducting State of κ-(ET)$_2$Cu[N(CN)$_2$]Br Studied by ^{13}C NMR: Evidence for Vortex-Core-Induced Nuclear Relaxation and Unconventional Pairing, Phys. Rev. Lett. **75**, 4122 (1995).

[44] K. Kanoda, K. Miyagawa, A. Kawamoto, and Y. Nakazawa, NMR relaxation rate in the superconducting state of the organic

conductor κ-(BEDT-TTF)$_2$Cu[N(CN)$_2$]Br, Phys. Rev. B **54**, 76 (1996).

[45] Y. Imamura, S. Ten-no, K. Yonemitsu, and Y. Tanimura, Structures and electronic phases of the bis(ethylenedithio)tetrathiafulvalene (BEDT-TTF) clusters and κ-(BEDT-TTF) salts: A theoretical study based on ab initio molecular orbital methods, J. Chem. Phys. **111**, 5986 (1999).

[46] T. Kawakami, T. Taniguchi, S. Nakano, Y. Kitagawa, and K. Yamaguchi, Theoretical studies on magnetic interactions in many types of organic donor salts: BEDT-TTF, BETS, TMTTF and TMTSF, Polyhedron **22**, 2051 (2003).

[47] D. Guterding, R. Valentí, and H. O. Jeschke, Influence of molecular conformations on the electronic structure of organic charge transfer salts, Phys. Rev. B **92**, 081109(R) (2015).

[48] T. Kobayashi and A. Kawamoto, Evidence of antiferromagnetic fluctuation in the unconventional superconductor λ-(BETS)$_2$GaCl$_4$ by ^{13}C NMR, Phys. Rev. B **96**, 125115 (2017).

[49] T. Kobayashi, H. Taniguchi, A. Ohnuma, and A. Kawamoto, Unconventional superconductivity in λ-(BETS)$_2$GaCl$_4$ probed by ^{13}C NMR, Phys. Rev. B **102**, 121106(R) (2020).

[50] T. Kobayashi, T. Ishikawa, A. Ohnuma, M. Sawada, N. Matsunaga, H. Uehara, and A. Kawamoto, Spin-density wave in the vicinity of superconducting state in λ-(BETS)$_2$GaBr$_x$Cl$_{4-x}$ probed by ^{13}C NMR spectroscopy, Phys. Rev. Research **2**, 023075 (2020).

[51] K. Kuroki, T. Kimura, R. Arita, Y. Tanaka, and Y. Matsuda, $d_{x^2-y^2}$- versus d_{xy}-like pairings in organic superconductors κ-(BEDT-TTF)$_2X$, Phys. Rev. B **65**, 100516(R) (2002).